

Effective temperatures of a driven, strongly anisotropic Brownian system

Min Zhang and Grzegorz Szamel*

Department of Chemistry, Colorado State University, Fort Collins, Colorado 80523, USA.

(Dated: July 31, 2021)

We use Brownian Dynamics computer simulations of a moderately dense colloidal system undergoing steady shear flow to investigate the uniqueness of the so-called effective temperature. We compare effective temperatures calculated from the fluctuation-dissipation ratios and from the linear response to a static, long wavelength, external perturbation along two directions: the shear gradient direction and the vorticity direction. At high shear rates, when the system is strongly anisotropic, the fluctuation-dissipation ratio derived effective temperatures are approximately wave-vector independent, but the temperatures along the gradient direction are somewhat higher than those along the vorticity direction. The temperatures derived from the static linear response show the same dependence on the direction as those derived from the fluctuation-dissipation ratio. However, the former and the latter temperatures are different. Our results suggest that the presently used formulae for effective temperatures may not be applicable for strongly anisotropic, driven systems.

PACS numbers: 82.70.Dd, 05.70.Ln, 83.50.Ax

I. INTRODUCTION

Temperature is one of the most important parameters describing a macroscopic system in equilibrium. In contrast, out of equilibrium, the very notion of temperature, its definition and its properties are still a subject of debate. This is true even for stationary nonequilibrium systems considered in this contribution. In principle, we can always define temperature in terms of average kinetic energy. It is not clear, however, whether such a definition leads to a parameter that has a more general significance. In addition, such a definition cannot be used for systems with overdamped stochastic dynamics (*e.g.* Brownian dynamics) [1].

In a seminal paper [2] Cugliandolo, Kurchan and Peliti proposed to define an effective, out-of-equilibrium temperature using a violation of a fluctuation-dissipation theorem. The starting point of their analysis was an earlier study [3] of the violation of the fluctuation-dissipation theorem in the low temperature phase of the spherical p -spin spin glass system. Building upon this study the authors of Ref. [2] showed that the ratio of the correlation and response functions, which in thermal equilibrium is equal to the temperature, has some properties of temperature even in out-of-equilibrium states. In particular, they showed that an effective temperature defined through the ratio of the correlation and response functions controls the direction of the heat flow.

Inspired by Ref. [2], Barrat, Berthier and Kurchan [4–6] investigated the effective temperature defined in terms of the violation of the fluctuation-dissipation theorem for a classic glass-forming system, the so-called Kob-Andersen [7] binary Lennard-Jones mixture, undergoing a steady shear flow. A stationary drive has some technical advantages compared to earlier studies of the effective

temperature for the same system undergoing aging [8]. The main one is that it can be expected that the system reaches a stationary non-equilibrium state in which time-translational invariance is restored. This fact makes easier both a computer simulation study and a theoretical investigation. A very interesting feature of a system consisting of particles, as opposed to mean-field spin systems, is that a great variety of response and correlation functions and the corresponding fluctuation-dissipation ratios can be defined. In principle, these different ratios could lead to a diverse set of effective temperatures. Then, it would be difficult to argue that any of these temperatures has a deeper meaning. However, Berthier and Barrat [6] showed that a class of fluctuation-dissipation ratios results in the same effective temperature. Furthermore, they showed that the same temperature is registered by a “thermometer”, *i.e.* a subsystem coupled to the simulated system.

In a related study Ono *et al.* [9] investigated a model sheared athermal system (zero-temperature foam). They considered a set of quantities that are equal to the temperature in equilibrium. Some of these quantities were based on static rather than dynamic linear response relations, and thus they were different from fluctuation-dissipation ratios considered in Refs. [2–6] from a fundamental point of view. Ono *et al.* found that the quantities they considered predicted the same value of effective temperature. Thus, these quantities could be used to define the effective temperature.

In a follow-up study O’Hern *et al.* [10] addressed the question of the relation between effective temperatures defined on the basis of static linear response relations [9] and the fluctuation-dissipation ratios [4–6]. They showed explicitly that in *most* cases these different definitions agreed over two and a half decades of effective temperature. However, in some cases they obtained different effective temperatures. The authors of Ref. [10] noted that it is not entirely clear whether a given pair of conjugate response and correlation function could be used to

*Electronic address: szamel@lamar.colostate.edu

define the effective temperature and which definition of the effective temperature (static or dynamic) should be used.

We briefly mention here a completely different system considered by Hayashi and Sasa [11]: a single Brownian particle moving in a tilted periodic potential. The advantage of this simple system is that many quantities can be calculated exactly [11, 12]. In particular, the diffusion coefficient and differential mobility can be calculated and their ratio can be used to define an effective temperature in close analogy with fluctuation-dissipation ratios of Refs. [2–6]. Interestingly, Hayashi and Sasa showed that the effective temperature obtained from the ratio of the diffusion coefficient and differential mobility plays the role of the usual temperature in the large scale description of their system. Consequently, they showed that, for this simple system, the fluctuation-dissipation ratio-derived temperature coincides with the temperature obtained from a long wavelength limit of a static linear response relation.

Many-particle driven systems for which various definitions of effective temperatures investigated so far have two common features. The first one, emphasized for example in Refs. [2, 4–6], is a separation of time scales: degrees of freedom evolving on short time scales seem to be thermalized with a different temperature than those evolving on the longest time scales. The latter degrees of freedom are thermalized with the effective temperature defined *via* the fluctuation-dissipation ratio. It should be noted that the importance of the time scale separation is somewhat less clear for the static definitions of the effective temperature. The second common feature is that driven systems considered in Refs. [4–6, 9, 10] were structurally isotropic. In particular, shear rates used in Ref. [6] were small enough for the steady state static structure factors in the flow, velocity gradient and vorticity directions to be identical within simulational uncertainty. Thus, there was no reason to expect that the effective temperature defined using wave-vector-dependent correlation functions would depend on the direction of the wave-vector and thus be anisotropic.

Here we consider a moderately dense model colloidal system undergoing a shear flow in the limit of high shear rates. As a result of the high shear rate our system is strongly anisotropic. In particular, the static structure factor in the velocity gradient direction is considerably larger than its equilibrium value [13] although no transition to a layered state [15] is observed. We test three definitions of effective temperature along two different directions, the velocity gradient direction and the vorticity direction. The first two definitions are based on the fluctuation-dissipation ratios. Specifically, the first definition is based on a violation of the Einstein relation between the friction coefficient and the self-diffusion coefficient, and the second definition is based on the violation of the fluctuation-dissipation relation between the transient response describing the change of the tagged particle density due to an external potential acting on

the tagged particle and the self-intermediate scattering function. The third definition is a static one based on the violation of the linear response relation describing the change of the density profile due to a static, long wavelength, external potential.

All three definitions allow us to calculate effective temperatures pertaining to different directions relative to the shear flow. In addition, the second definition allows us to calculate effective temperatures corresponding to different wave-vectors. We find that the effective temperatures derived from the fluctuation-dissipation ratios are wave-vector independent, but at high shear rates the temperatures along the velocity gradient direction are somewhat larger than those along the vorticity direction.

The dependence of the effective temperatures on the direction correlates with the fact that at high shear rates the system is strongly anisotropic. In addition, we find that the effective temperatures obtained from the static linear response relation show the same dependence on the direction as those derived from the fluctuation-dissipation ratios. However, the effective temperatures obtained from the static linear response relation are different from those derived from the fluctuation-dissipation ratios. Finally, we show that if the static linear response definition is generalized to shorter wavelengths (*i.e.* to more rapidly varying in space periodic potentials), the resulting effective temperatures have complicated wave-vector and direction dependence.

The paper is organized as follows. In the next section, Sec. II, we describe the details of the simulation. We discuss the structure of the sheared system in Sec. III; in particular, we show that at high shear rates the system is strongly anisotropic. In Secs. IV, V and VI we present effective temperatures determined using the three different definitions. We close the paper with a short discussion presented in Sec. VII. In the appendix we examine the wave-vector dependence of the effective temperatures defined through the static linear response relation.

II. SIMULATION DETAILS

We simulated one of the systems investigated in an earlier publication [16]. Briefly, the system consists of $N = 1372$ spherical colloidal particles. We used the screened Coulomb potential originally introduced by Rastogi *et al* [15]:

$$V(r) = A \frac{\exp(-\kappa(r - \sigma))}{r}, \quad (1)$$

with $A = 475k_B T \sigma$ and $\kappa \sigma = 24$. The cutoff distance was 3σ . We simulated the system at dimensionless densities, $(N/V)\sigma^3 \equiv n\sigma^3$ equal to 0.408 (V is the system's volume). We previously established [16] that this density corresponds to an effective hard-sphere volume fraction equal to 0.43. Thus, our system is moderately dense.

We performed Brownian dynamics simulations. The equation of motion for the i th particle is,

$$\dot{\mathbf{r}}_i = \dot{\gamma} y_i \hat{\mathbf{e}}_x - \frac{1}{\xi_0} \partial_{\mathbf{r}_i} \sum_{j \neq i} V(|\mathbf{r}_i - \mathbf{r}_j|) + \eta_i(t) \quad (2)$$

where $\dot{\gamma}$ is the shear rate, y_i is the coordinate of particle i along y direction, $\hat{\mathbf{e}}_x$ is the unit vector along the x direction, ξ_0 is the friction coefficient of an isolated particle, and the random noise η_i satisfies the fluctuation-dissipation theorem,

$$\langle \eta_i(t) \eta_j(t') \rangle = 2D_0 \delta(t - t') \delta_{ij} I. \quad (3)$$

In equation (3), I is the unit tensor and the diffusion coefficient $D_0 = k_B T / \xi_0$ where k_B is Boltzmann's constant. We will present the results in terms of reduced units with σ and σ^2 / D_0 being the units of length and time, respectively.

The equations of motion, Eq. (2), were solved with Lees-Edwards boundary conditions for shear rates $\dot{\gamma} = 2, 5, 10$ and 20 . To solve the equations of motion we used a second order Brownian dynamics algorithm [17] with a time step of 10^{-4} for shear rates 2 and 5 , and a time step of 5×10^{-5} for shear rates 10 and 20 .

III. STRUCTURE OF THE SHEARED SYSTEM

A fluid's structure is usually discussed in terms of its pair distribution function. Under shear, the pair distribution function $g(\mathbf{r})$,

$$g(\mathbf{r}) = \frac{V}{N(N-1)} \left\langle \sum_{i \neq j}^N \delta(\mathbf{r} - \mathbf{r}_j + \mathbf{r}_i) \right\rangle \quad (4)$$

is anisotropic (hereafter the brackets $\langle \dots \rangle$ denote the non-equilibrium steady state average). The anisotropic pair distribution is somewhat difficult to visualize and usually only its two lowest order projections on spherical harmonics are monitored [18]:

$$g^s(r) = \frac{1}{4\pi} \int d\hat{\mathbf{r}} g(\mathbf{r}), \quad g_+(r) = \frac{15}{4\pi} \int d\hat{\mathbf{r}} \hat{x} \hat{y} g(\mathbf{r}). \quad (5)$$

Here we follow notation introduced by Hess and Hanley [19]: $g^s(r)$ denotes the isotropic component of the pair distribution function, which in the absence of the shear flow reduces itself to the familiar equilibrium pair distribution function $g_{eq}(r)$. Next, $g_+(r)$ denotes the projection of the pair distribution function onto $\hat{x}\hat{y}$. In principle, the anisotropic pair distribution $g(\mathbf{r})$ can be reconstructed from the projections

$$g(\mathbf{r}) = g^s(r) + g_+(r) \hat{x} \hat{y} + \dots, \quad (6)$$

but, in practice, for high shear rates the expansion indicated above is slowly convergent and the higher order terms, indicated by dots in Eq. (6), are important [20].

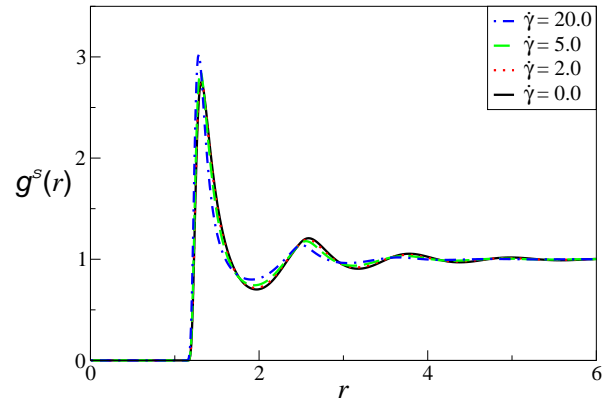


FIG. 1: (Color online) The isotropic component of the pair distribution function, $g^s(r)$, as a function of the particle separation, r , for different shear rates.

In the limit of low shear rates $g^s = g_{eq} + o(\dot{\gamma})$, g_+ is proportional to $\dot{\gamma}$ and all projections other than g^s and g_+ are $o(\dot{\gamma})$. In addition to being the dominant small $\dot{\gamma}$ correction to the equilibrium pair distribution, the importance of g_+ comes from the fact that for pair-wise additive interactions it determines the xy component of the interaction contribution to the stress tensor, σ_{xy} ,

$$\sigma_{xy} = \frac{n^2 4\pi}{2 \cdot 15} \int_0^\infty dr r^3 \frac{dV(r)}{dr} g_+(r) \quad (7)$$

and, as a consequence, the non-linear viscosity $\eta(\dot{\gamma}) = \sigma_{xy} / \dot{\gamma}$.

We show g^s and g_+ in Figs. 1 and 2. With increasing shear rate the isotropic component, g^s , changes little whereas the amplitude of g_+ systematically increases. The inset in Fig. 2 shows that this increase of g_+ is sub-linear in $\dot{\gamma}$. This fact is a reflection of the well-known shear thinning phenomenon: sub-linear increase of g_+ leads to a sub-linear increase of the xy component of the stress tensor and a decrease of the non-linear viscosity with increasing shear rate.

While the isotropic component of the pair correlation function g^s changes little with increasing shear, at the largest shear rate investigated, $\dot{\gamma} = 20$, the first anisotropic component g_+ is comparable to g^s . In fact, although it is not evident from Fig. 2, the system is strongly anisotropic already at $\dot{\gamma} = 5$. The first evidence of this anisotropy can be obtained by investigating the static structure factor $S(k)$,

$$S(\mathbf{k}) = \frac{1}{N} \langle \rho(\mathbf{k}) \rho(-\mathbf{k}) \rangle, \quad \rho(\mathbf{k}) = \sum_{i=1}^N \exp(-i\mathbf{k} \cdot \mathbf{r}_i), \quad (8)$$

along specific directions in \mathbf{k} space.

In Fig. 3 we show the structure factor along two different directions: the velocity gradient direction $\hat{\mathbf{e}}_y$ and the vorticity direction $\hat{\mathbf{e}}_z$. We see that the first peak

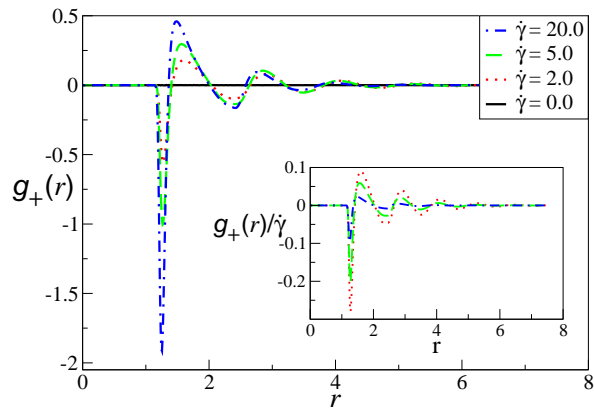


FIG. 2: (Color online) The first anisotropic component of the pair distribution function, $g_+(r)$, as a function of the particle separation, r , for different shear rates. The inset shows $g_+(r)/\dot{\gamma}$.

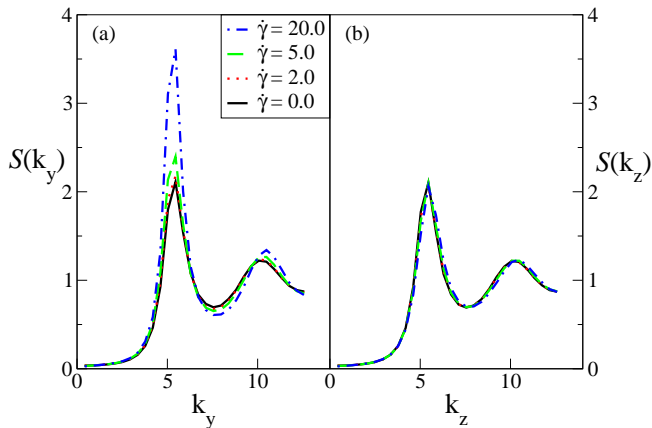


FIG. 3: (Color online) The structure factor, $S(\mathbf{k})$, for \mathbf{k} along two different directions for different shear rates. (a) gradient direction, $\hat{\mathbf{e}}_y$. (b) vorticity direction, $\hat{\mathbf{e}}_z$.

of the structure factor along the gradient direction increases strongly with shear rate starting at a shear between $\dot{\gamma} = 2$ and $\dot{\gamma} = 5$. In contrast, the structure factor along the vorticity direction shows almost no shear rate dependence. Similar behavior was seen before for a system under oscillatory shear flow [14]. The increase of the structure factor along the velocity gradient direction can be interpreted in terms of local ordering into a layered-like structure [15].

To investigate the cross-over between strong shear rate dependence of the structure factor along the gradient direction and weak shear rate dependence along the vorticity direction it is useful to visualize the structure factor in some planes in the wave-vector space. We investigated the shear rate dependence of the structure factor

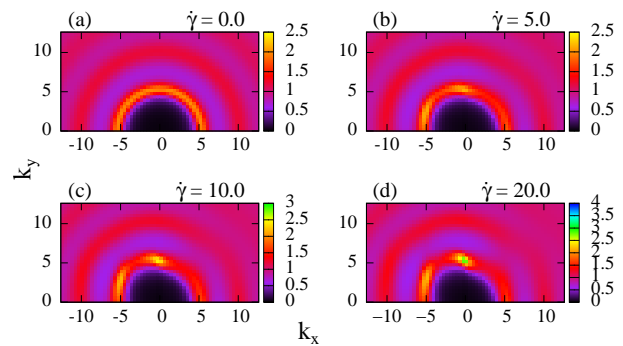


FIG. 4: (Color online) The structure factor, $S(\mathbf{k})$, in the velocity-gradient plane, for different shear rates.

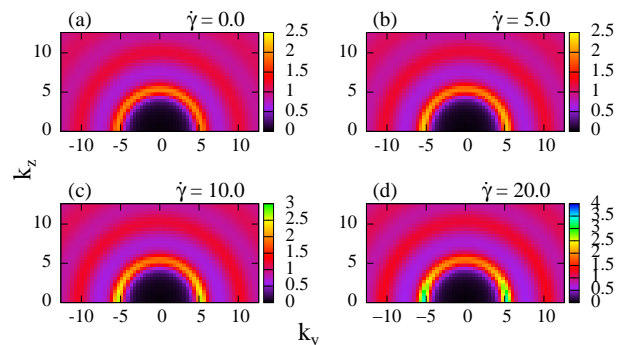


FIG. 5: (Color online) The structure factor, $S(\mathbf{k})$, in the gradient-vorticity plane, for different shear rates.

in two planes, the flow-velocity gradient plane (x - y) and the gradient-vorticity (y - z) plane. Fig. 4 shows that the increase of the structure factor along the velocity gradient direction is quite localized in the flow-velocity gradient plane. Moreover, we note that at the highest shear rate the whole ring-like pattern becomes strongly deformed. In contrast, Fig. 5 shows that in the velocity gradient-vorticity plane the transition from strong increase of the structure along the gradient direction to almost shear rate independent structure factor along the vorticity direction is more gradual. In addition, in the velocity gradient-vorticity plane the ring-like structure is still quite un-deformed even at the highest shear rate.

To summarize, in this section we showed that at high shear rates the steady-state system is strongly anisotropic.

IV. EFFECTIVE TEMPERATURE: EINSTEIN RELATION

According to the celebrated Einstein relation, the mean-square displacement of the tagged particle is related to the tagged particle motion under the influence of a weak external potential acting on the tagged particle only. Specifically, for a system in equilibrium, in the long

time limit we can define the equilibrium self-diffusion coefficient D via the tagged particle mean square displacement,

$$\lim_{t \rightarrow \infty} \frac{1}{t} \left\langle |\mathbf{r}_i(t) - \mathbf{r}_i(0)|^2 \right\rangle_{eq} = 6D_{eq}, \quad (9)$$

where the brackets $\langle \dots \rangle_{eq}$ denote the equilibrium average. In addition, we can define the equilibrium self-mobility coefficient μ via the systematic displacement of the tagged particle under the influence of the weak external force of magnitude F_0 acting along an arbitrary direction specified by the unit vector $\hat{\mathbf{f}}$,

$$\lim_{F_0 \rightarrow 0} \lim_{t \rightarrow \infty} \frac{1}{tF_0} \left\langle (\mathbf{r}_i(t) - \mathbf{r}_i(0)) \cdot \hat{\mathbf{f}} \right\rangle_{eq}^{F_0} = \mu_{eq}, \quad (10)$$

where $\langle \dots \rangle_{eq}^{F_0}$ denotes an average in a system without shear, subjected to a constant force acting on the tagged particle.

D_{eq} and μ_{eq} are connected via the so-called Einstein relation involving the system's temperature T ,

$$D_{eq} = T\mu_{eq}. \quad (11)$$

For a steady state system under shear both the self-diffusion coefficient and the self-mobility coefficient depend on the shear rate. We note here that, for colloidal systems under oscillatory shear, the shear rate dependence of the former was studied over two decades ago in experiments [21] and computer simulations [14]. These studies were followed by theoretical studies of self-diffusion in semi-dilute [22] and concentrated [23] colloidal systems under steady shear. In the former work, the self-mobility was also studied and the violation of the Einstein relation (11) was noted. The realization that Eq. (11) is violated was not followed, however, by the crucial step of the identification of an effective temperature. Berthier and Barrat [6, 24] made this last step, turned Eq. (11) around, defined and calculated the effective temperature

$$T_{eff} = D/\mu. \quad (12)$$

It should be emphasized that both quantities at the right-hand-side of Eq. (12) depend on the shear rate $\dot{\gamma}$ but in a slightly different way. It is this last fact that gives rise to a non-trivial effective temperature.

Since our system is anisotropic, we investigated two different effective temperatures based on the violation of Eq. (11) along two different directions, the gradient direction and the vorticity direction,

$$T_{eff}^y = D_{yy}/\mu_{yy}, \quad (13)$$

$$T_{eff}^z = D_{zz}/\mu_{zz}. \quad (14)$$

Here D_{yy} and D_{zz} are the diagonal components of the self-diffusion tensor along the gradient and vorticity directions, respectively,

$$\lim_{t \rightarrow \infty} \frac{1}{t} \left\langle (\alpha_i(t) - \alpha_i(0))^2 \right\rangle = 2D_{\alpha\alpha}, \quad (15)$$

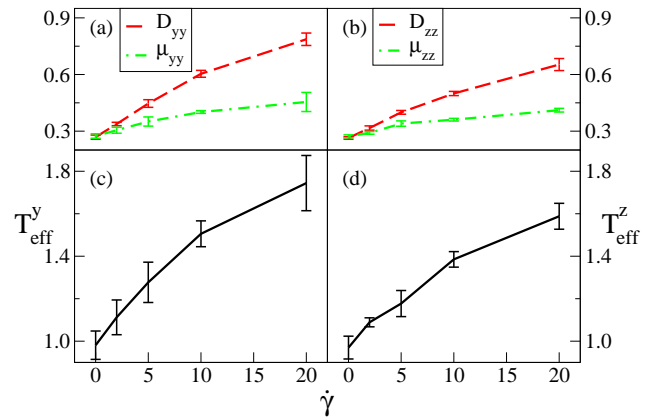


FIG. 6: (Color online) (a-b): shear rate dependence of the diagonal components of the self-diffusion and mobility tensors. Note that in equilibrium, *i.e.* for $\dot{\gamma} = 0$, for our value of temperature, $T = 1$, the self-diffusion and the mobility coefficients are equal, $D_{eq} = \mu_{eq}$. (c-d): shear rate dependence of the effective temperature obtained from the self-diffusion and mobility tensors. (a) and (c): gradient direction, $\hat{\mathbf{e}}_y$. (b) and (d): vorticity direction, $\hat{\mathbf{e}}_z$.

where $\alpha = y$ or $\alpha = z$. Furthermore, in Eqs. (13-14) μ_{yy} and μ_{zz} are the diagonal elements of the self-mobility tensor

$$\lim_{F_0 \rightarrow 0} \lim_{t \rightarrow \infty} \frac{1}{tF_0} \langle (\alpha_i(t) - \alpha_i(0)) \rangle^{F_0} = \mu_{\alpha\alpha}, \quad (16)$$

where, again, $\alpha = y$ or $\alpha = z$, and the weak external force of magnitude F_0 is applied on the tagged particle in the direction α .

The elements of the self-diffusion tensor can be easily calculated. In contrast, an evaluation of the elements of the self-mobility tensor is a little more challenging. We followed the procedure described in Ref. [6] and introduced a constant force acting on 686 randomly selected particles of the system, with the force in the positive direction along the relevant axis for 343 particles and the force in the negative direction for the remaining 343 particles. The average systematic displacement of these particles, weighted by the sign of the force, is a good approximation for $\langle (\alpha_i(t) - \alpha_i(0)) \rangle$ and can be used to calculate $\mu_{\alpha\alpha}$. We checked this assertion by re-doing this calculation with a constant force acting on 340 randomly selected particles of the system. As expected, the statistics was worse, but the results were compatible with the calculation using a constant force acting on 686 particles.

The results are presented in Fig. 6. The upper panels of this figure show that both the diagonal elements of the self-diffusion tensor and the diagonal elements of the self-mobility tensor increase with increasing shear rate. Both quantities are somewhat larger along the gradient direction than along the vorticity direction. We note that for a system under an oscillatory shear an early simulation of Xue and Grest [14] found the opposite behavior for the elements of the self-diffusion tensor. In contrast, for a system under steady shear a theoretical study of Indrani

and Ramaswamy [23] found that the diagonal elements of the self-diffusion tensor along the gradient direction was larger than those along the vorticity direction. This qualitatively agrees with the results for the elements of the self-diffusion tensor showed in Fig. 6. It should be emphasized, however, that in Ref. [23] the violation of the Einstein relation was neglected and thus Indrani and Ramaswamy's approach cannot describe the difference between self-diffusion and self-mobility tensors.

The lower panels of Fig. 6 show that, as found in earlier investigations, the effective temperature increases with increasing shear rate. The temperatures along the gradient and vorticity directions are quite close, but the one along the gradient direction is systematically somewhat larger than the one along the vorticity direction. We should note, however, that the uncertainty of these effective temperatures prevents us from making a definitive statement that the two temperatures are different.

V. EFFECTIVE TEMPERATURE: FDR INVOLVING THE SELF-INTERMEDIATE SCATTERING FUNCTION

According to the standard fluctuation-dissipation relation, in equilibrium the susceptibility describing a time-delayed change of the tagged particle density is proportional to the self-intermediate scattering function,

$$\chi_{s,eq}(k;t) = \frac{1}{T} [1 - F_{s,eq}(k;t)]. \quad (17)$$

Here $\chi_{s,eq}(k;t)$ is the susceptibility describing the change of the Fourier component k of the tagged particle density due to a weak external force acting on the tagged particle,

$$\chi_{s,eq}(k;t) = \frac{\partial}{\partial h} \langle \exp[i\mathbf{k} \cdot \mathbf{r}_i(t)] \rangle_{eq}^h \Big|_{h=0} \quad (18)$$

where $\langle \dots \rangle_{eq}^h$ denotes an average calculated in a system that was in equilibrium at $t = 0$ and subsequently was subjected to a constant in time force \mathbf{F}_i^{ext} acting on the tagged particle only,

$$\mathbf{F}_i^{ext} = -\partial_{\mathbf{r}_i} [2h \cos(\mathbf{k} \cdot \mathbf{r}_i)].$$

Furthermore, $F_{s,eq}(k;t)$ in Eq. (17) is the equilibrium self-intermediate scattering function,

$$F_{s,eq}(k;t) = \langle \exp[i\mathbf{k} \cdot (\mathbf{r}_i(t) - \mathbf{r}_i(0))] \rangle. \quad (19)$$

For a system undergoing a steady shear flow, the relation (17) is violated. Following [6] we define an effective temperature through the violation of this relation,

$$T_{eff}^\alpha = \frac{1 - F_s(k_\alpha; t)}{\chi_s(k_\alpha; t)} \quad (20)$$

All quantities at the right-hand-side of Eq. (20) are calculated for a system undergoing a steady shear. Specifi-

cally, $F_s(k_\alpha; t)$ is the steady state self-intermediate scattering function. Moreover, $\chi_s(k_\alpha; t)$ describes the time-delayed change of the tagged particle density,

$$\chi_s(k; t) = \frac{\partial}{\partial h} \langle \exp[i\mathbf{k} \cdot \mathbf{r}_i(t)] \rangle^h \Big|_{h=0}, \quad (21)$$

where $\langle \dots \rangle^h$ denotes an average calculated in a system that was undergoing a steady shear at $t = 0$, and subsequently was subjected to a constant in time force acting on the tagged particle. It should be noted that the effective temperatures in definition (20), in addition to the dependence on the direction of the force, $\alpha = y, z$, can also depend on the magnitude of the wave-vector (to simplify notation this possible dependence is not indicated explicitly). As discussed in the Introduction, the authors of Ref. [6] found that, for a supercooled system under weak shear, the effective temperatures defined through Eq. (20) does not depend on the wave-vector.

The calculation of the self-intermediate scattering function is straightforward. In contrast, it is more difficult to calculate the susceptibility. We followed the procedure described in Ref. [6]. Specifically, we considered a system with a constant force imposed on 686 randomly selected particles of the system, with the force in the positive direction along the relevant axis for 343 particles and the force in the negative direction for the remaining 343 particles. Furthermore, in order to evaluate the susceptibility using the unperturbed trajectories, we followed a recently introduced approach [25] and we performed the derivative in Eq. (21) *before* taking the average. This necessitates solving additional equations of motion for quantities $\partial \mathbf{r}_i / \partial h$ [25], but it allowed us to calculate the susceptibility from one long, unperturbed trajectory. It should be noted that, in contrast to the calculation described in Ref. [25], we did not have to perform several independent runs. This simplification follows from the fact that while in Ref. [25] a response of an aging system was studied, we are interested in a response of a steady state system.

In Fig. 7 we show parametric plots of the susceptibility versus the correlation function for several wave-vectors along the y and z axes at the highest shear rate, $\dot{\gamma} = 20$. In plots of this type the effective temperature is the (minus) of the inverse slope of the data. Moreover, short times correspond to the lower right corner and long times to the upper left corner of the plot. One can see from Fig. 7 that at short times the fluctuation-dissipation (17) is obeyed. In contrast, at long times an effective temperature higher than the heat bath temperature is observed. Notice that at long times, for a given direction, the slopes of the lines fitted to the data obtained at different magnitudes of the wave-vectors seem very close. This agrees with the findings of Ref. [6]. In contrast, the slopes of the lines fitted to the data obtained at two different directions are different.

The results of the analysis of parametric plots at all shear rates investigated are presented in Fig. 8. In agreement with the behavior found from the analysis of

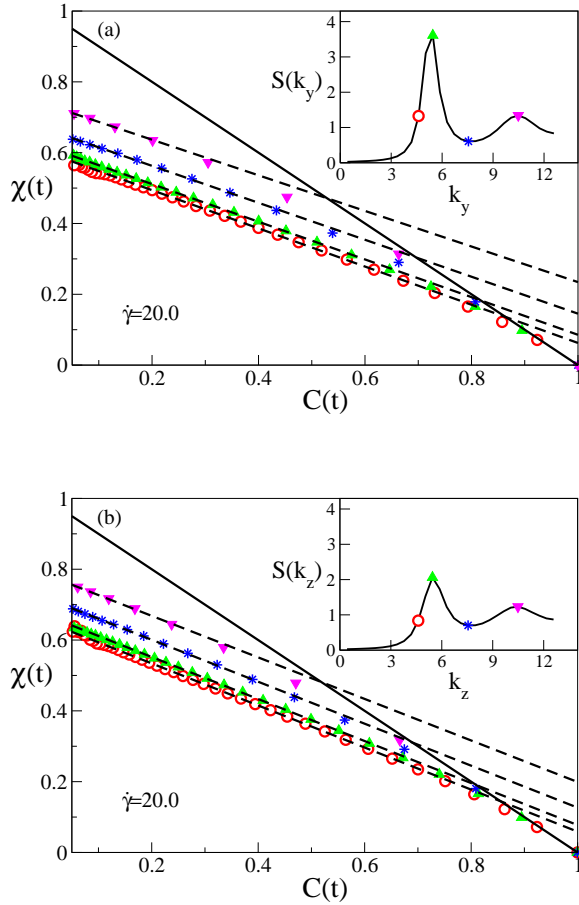


FIG. 7: (Color online) Parametric plots $\chi_s(k_\alpha; t)$ vs. $F_s(k_\alpha; t)$ for wave-vectors along two directions. (a) gradient direction, \hat{e}_y . (b) vorticity direction, \hat{e}_z . The magnitudes of the wave-vectors are $k_\alpha = 4.61, 5.45, 7.55$ and 10.48 , listed from bottom to top. The solid lines have slopes equal to $-1/T = -1$. The dashed lines have slopes equal to $-1/T_{eff}^\alpha$. The insets indicate the magnitudes of the wave-vectors in relation to the steady state structure factors for wave-vectors along the gradient and vorticity directions. Recall that at this high shear rate the steady state structure factors along these directions are quite different, see Fig. 3.

the violation of the Einstein relation, we find that that in both directions and at all wave-vectors the effective temperatures increase with increasing shear rate. The temperatures obtained from different magnitudes of the wave-vectors are reasonably consistent. This agrees with the finding of Berthier and Barrat [6]. As found in the previous section, temperatures obtained from the external force along the gradient and vorticity directions are close, but the one along the gradient direction is systematically larger than the one along the vorticity direction.

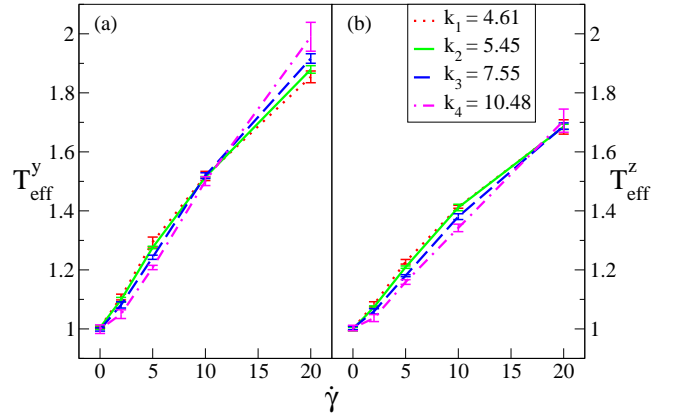


FIG. 8: (Color online) Shear rate dependence of effective temperatures obtained from the violation of the fluctuation-dissipation relation involving the self-intermediate scattering function. (a): gradient direction, \hat{e}_y . (b): vorticity direction, \hat{e}_z .

VI. EFFECTIVE TEMPERATURE: STATIC LINEAR RESPONSE DEFINITION

For a system in equilibrium, the static structure factor plays the role of the response function: the change of the average density due to a weak, static, periodic in space, external potential,

$$V(\mathbf{r}) = V_0 \sin(\mathbf{q} \cdot \mathbf{r}), \quad (22)$$

which has been turned on at $t = -\infty$, is given by the following well known relation:

$$\delta n(\mathbf{r}) = -\frac{n S_{eq}(q)}{T} V_0 \sin(\mathbf{q} \cdot \mathbf{r}) \quad (23)$$

where T is the system's temperature and $S_{eq}(q)$ is the equilibrium structure factor.

The main finding of Ref. [10] is that the effective temperature obtained from the long wavelength (*i.e.* small wave-vector) limit of *some* linear response relations agrees with that obtained from the fluctuation-dissipation ratios. Inspired by this result here we use the relation (23) to define an effective temperature. Specifically, we assume a sheared, stationary suspension, impose a slowly varying external potential (22) (we use the smallest wave-vector allowed by periodic boundary conditions), wait a time long enough for the system to reach a new stationary state, and measure the density change due to the external potential. We use two different strengths of the effective potential (*i.e.* two different values of V_0) to extrapolate to the linear response limit implicit in Eq. (23). In the limit of weak external potential the density change is proportional to V_0 ,

$$\delta n(\mathbf{r}) = -n a(\mathbf{q}) V_0 \sin(\mathbf{q} \cdot \mathbf{r}) \quad (24)$$

where we made explicit the fact that under shear the density change depends on the orientation of the vector \mathbf{q}

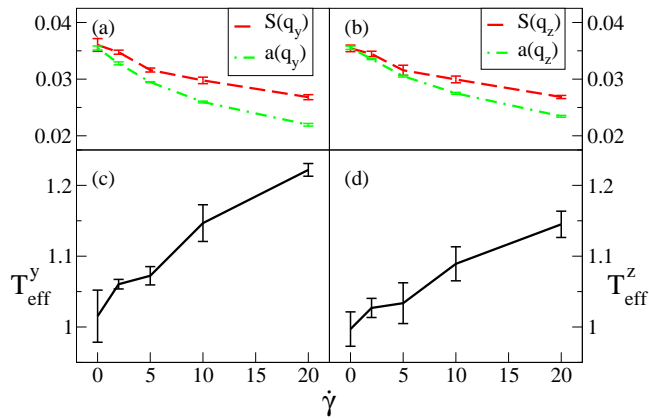


FIG. 9: (Color online) (a-b): shear rate dependence of the steady state structure factor $S(q_\alpha)$ and the response coefficient $a(q_\alpha)$, $\alpha = y, z$, where q_α is the smallest non-zero wave-vector allowed by the periodic boundary conditions, $q_y = q_z = 0.42$. (c-d): shear rate dependence of the effective temperature obtained from the static linear response. (a) and (c): gradient direction, $\hat{\mathbf{e}}_y$. (b) and (d): vorticity direction, $\hat{\mathbf{e}}_z$.

with respect to the shear flow. Next, we use the following generalization of the relation (23) to extract the static effective temperature:

$$T_{\text{eff}}^\alpha = \frac{S(q_\alpha)}{a(q_\alpha)} \quad (25)$$

It should be noted that the definition (25) involves the shear rate dependent, anisotropic structure factor $S(\mathbf{q})$. This agrees with the static definition adopted in Ref. [10]. Thus, the static effective temperature (25) is a ratio of two shear rate-dependent quantities.

In contrast to the procedure adopted in Ref. [10] we did not monitor the time dependent (transient) density change after the external potential was turned on, and thus do not obtain the static effective temperature from an intercept of a parametric plot of the response (*i.e.* the density change) as a function of the time dependent density correlation function. However, our definition of the effective temperature is equivalent to that used in Ref. [10].

In Fig. 9 we present the shear rate dependence of the structure factor and the linear response coefficient a . Since we are interested in the response to a long wavelength perturbation, both quantities are shown for the smallest wave-vector compatible with periodic boundary conditions, $q_y = q_z = 0.42$. While both quantities decrease with increasing shear rate, the coefficient a has a somewhat stronger dependence on $\dot{\gamma}$. As a result, as shown in lower panels in Fig. 9, the effective temperatures calculated for the perturbation along the gradient and vorticity directions increase with shear rate. The effective temperature along the gradient direction is larger than that along the vorticity direction. This agrees with the behavior obtained from the Einstein relation and the

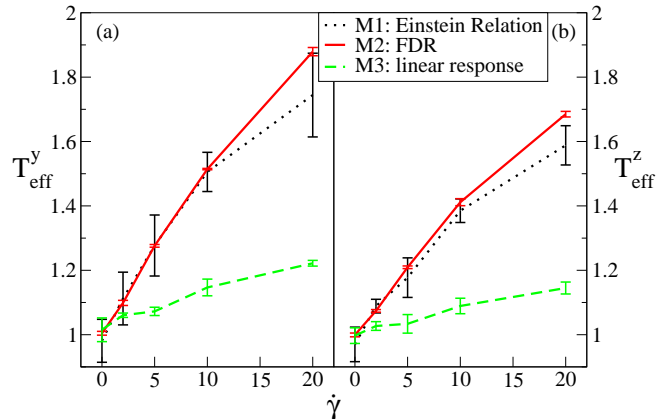


FIG. 10: (Color online) Comparison of the shear rate dependence of effective temperatures obtained using three different definitions. Dotted line: Einstein relation; solid line: violation of the fluctuation-dissipation relation for the self-intermediate scattering function at the wave-vector corresponding to the peak position of the structure factor; dashed line: static linear response to a long wavelength perturbation. (a) gradient direction, $\hat{\mathbf{e}}_y$. (b) vorticity direction, $\hat{\mathbf{e}}_z$.

fluctuation-dissipation ratios. However, the values of the effective temperature obtained from static linear response are different than those obtained from the fluctuation-dissipation ratios.

VII. DISCUSSION

To investigate the uniqueness of the notion of the so-called effective temperature of a driven colloidal system we studied three definitions of such a temperature. The main results are summarized in Fig. 10.

We evaluated the effective temperature obtained from the violation of the Einstein relation [6] and the effective temperature obtained from the violation of the fluctuation-dissipation relation involving the self-intermediate scattering function [6]. The latter definition allows to calculate the effective temperature at different wave-vectors. Formally, the former definition can be considered as the limiting case of the latter one for vanishing magnitude of the wave-vector. Berthier *et al.* [6] found that these two definitions resulted in compatible values of the effective temperatures. Our results suggest that at higher shear rates, when the system is anisotropic, the two definitions give the same result along the gradient direction and along the vorticity direction. However, the effective temperatures along the gradient direction are somewhat larger than those along the vorticity direction.

In addition, we investigated a definition of the effective temperature based on a static linear response relation. The motivation for this was two-fold. First, similar relations were investigated by O'Hern *et al.* [10].

Second, Hayashi and Sasa [11] found that for their simple, single particle system, the effective temperature defined through a fluctuation-dissipation ratio determines the response of the system to a long wavelength potential. We found that the effective temperatures obtained from the static linear response relation were different from those obtained from violation of the Einstein relation and of the fluctuation-dissipation relation involving the self-intermediate scattering function. However, in the long wavelength limit static linear response derived effective temperatures had the same dependence on the direction: temperatures along the gradient direction were somewhat larger than those along the vorticity direction. In the appendix we extended the static linear response definition of the effective temperature to shorter wavelength perturbations. As shown in Fig. 12, at shorter wavelengths (larger wave-vectors) the static linear response relation leads to a variety of different effective temperatures, and in some cases with dependence on the direction opposite to that shown in Fig. 10.

It would be interesting to repeat our numerical investigation for a more strongly interacting system with a clear separation of time scales. To this end, however, one would have to use a mixture (possibly, Kob-Andersen binary Lennard-Jones mixture) because we found that our single component system forms layers at high density and large shear rates (as was first reported in Ref. [15]).

It would also be interesting to develop some theoretical understanding of the definitions of the effective temperature investigated here. First steps in this direction have already been taken [24, 26]. It is still not clear, however, when one has to use a fluctuation-dissipation based definition of the effective temperature and when one can use a static linear response based definition for a many-particle, strongly interacting, sheared system.

More generally, it would be worthwhile to establish what, if any, properties of a many-particle, strongly interacting, sheared system are influenced by which definition of the effective temperature. Again, first steps in this direction have already been taken [27]. We would like to mention here a very interesting result concerning driven systems with Newtonian dynamics: alignment of particles in a shear flow depends on whether kinetic or configurational [1] temperature is thermostated [28].

The main conclusion from our study is that for a strongly driven, anisotropic system presently used, definitions of the effective temperature may not give a unique, direction-independent result. It is, therefore, imperative that the realms of validity and importance are established for these definitions. Only then we will be able to fully assess the relevance of the existing definitions.

Acknowledgments

We thank E. Flenner for comments on the manuscript and gratefully acknowledge the support of NSF Grant No. CHE 0909676.

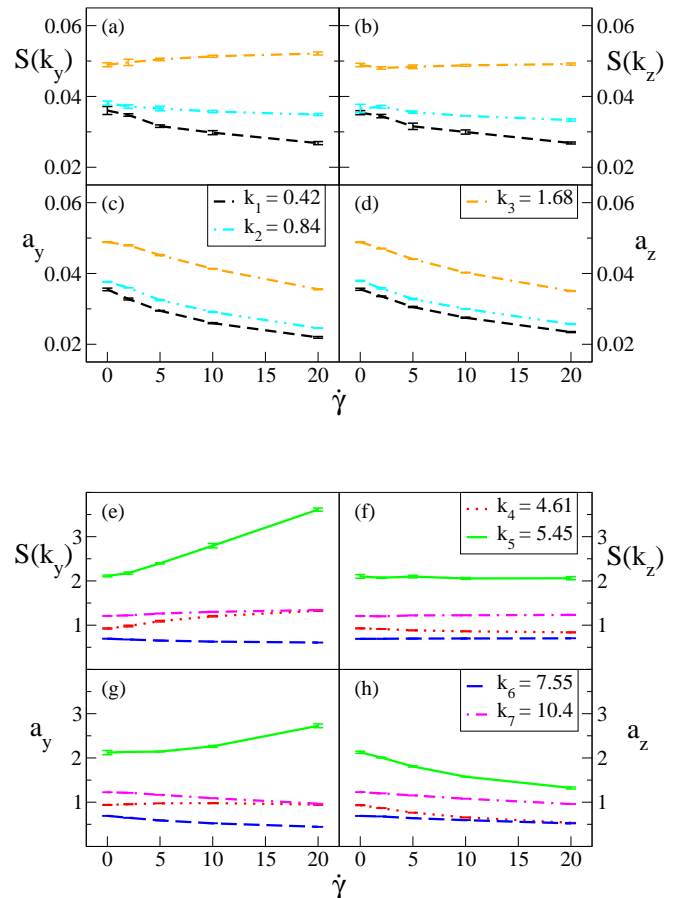


FIG. 11: (Color online) (a-b) and (e-f): shear rate dependence of the structure factor. (c-d) and (g-h): shear rate dependence of the linear response coefficient. (a), (c), (e) and (g): gradient direction, \hat{e}_y . (b), (d), (f) and (h): vorticity direction, \hat{e}_z . (a-d) show smaller wave-vectors and (e-h) show larger wave-vectors.

Appendix

Here we generalize the static linear response based definition of effective temperature. The main motivation for this generalization is that, as shown in Fig. 10, the static linear response to a long wavelength perturbation gives effective temperatures that are different from those obtained using the fluctuation-dissipation ratios. This difference prompted us to check whether it is still present at larger wave-vectors.

Effective temperatures presented in this section were obtained using relation (25) generalized to larger wave-vectors:

$$T_{\text{eff}}^{\alpha} = \frac{S(k_{\alpha})}{a(k_{\alpha})} \quad (26)$$

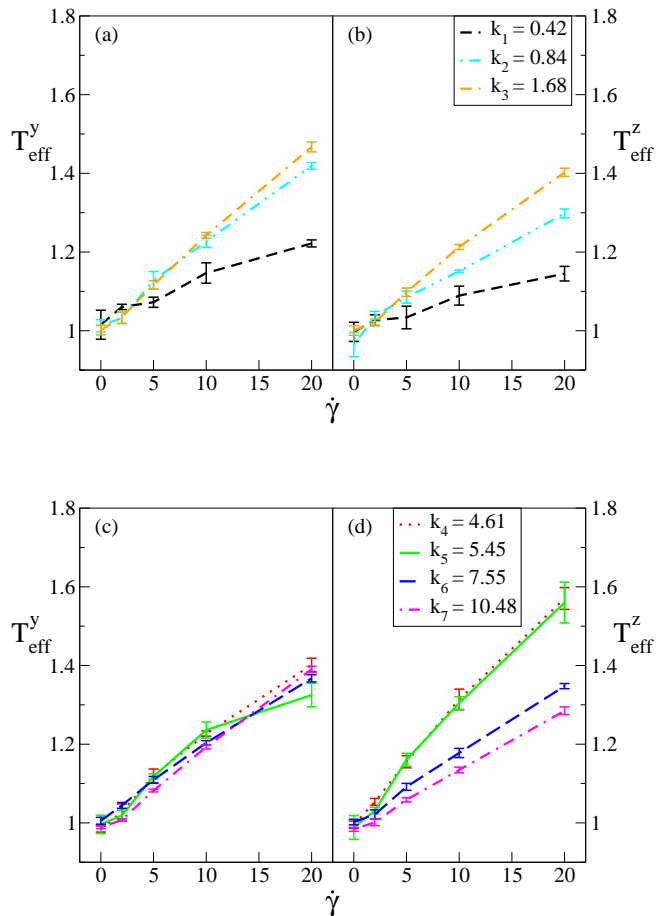


FIG. 12: (Color online) Shear rate dependence of the static effective temperature at a number of wave-vectors. (a) and (c) : gradient direction, \hat{e}_y . (b) and (d): vorticity direction, \hat{e}_z . (a-b) show smaller wave-vectors and (c-d) show larger wave-vectors.

In Eq. (26) the effective temperature may depend on the wave-vector.

In Figs. 11 and 12 we show the shear rate dependence of the structure factor, linear response coefficient, and effective temperature for different wave-vectors along two directions, the gradient direction and the vorticity direction. We find that effective temperature as defined through Eq. (26) depends significantly on the wave-vector. In particular, whereas at small wave-vectors temperatures along the gradient direction are somewhat larger than those along the vorticity direction, at some of the larger wave-vectors this ordering is reversed. Our finding emphasizes the need for some theoretical understanding of the static linear response definition of effective temperature.

-
- [1] An alternative is the so-called configurational temperature [H.H. Rugh, Phys. Rev. Lett. **78**, 772 (1997)]. This temperature can be used for Brownian systems, see J. Ennisa and D.J. Evans, Molecular Simulation **26**, 147 (2001).
- [2] L.F. Cugliandolo, J. Kurchan, and L. Peliti, Phys. Rev. E **55**, 3898 (1997).
- [3] L.F. Cugliandolo and J. Kurchan, Phys. Rev. Lett. **71**, 173 (1993).
- [4] L. Berthier, J.-L. Barrat and J. Kurchan, Phys. Rev. E **61**, 5464 (2000).
- [5] J.-L. Barrat and L. Berthier, Phys. Rev. E **63**, 012503 (2000).
- [6] L. Berthier and J.-L. Barrat, Phys. Rev. Lett. **89**, 095702 (2002); J. Chem. Phys. **116**, 6228 (2002).
- [7] W. Kob and H.C. Andersen, Phys. Rev. E **51**, 4626 (1995); Phys. Rev. E **52**, 4134 (1995).
- [8] W. Kob and J.-L. Barrat, Phys. Rev. Lett. **78**, 4581 (1997).
- [9] I. Ono *et al*, Phys. Rev. Lett. **89**, 095703 (2002).
- [10] C.S. O'Hern, A.J. Liu, and S.R. Nagel, Phys. Rev. Lett. **93**, 165702 (2004).
- [11] K. Hayashi and S. Sasa, Phys. Rev. **69**, 066119 (2004).
- [12] See also Reimann *et al.*, Phys. Rev. Lett. **87**, 010602 (2001).
- [13] The increase of the steady state structure factor along the velocity gradient direction was also seen in model suspensions undergoing oscillatory shear, [14].
- [14] W. Xue and G. Grest, Phys. Rev. A **40**, 1709 (1989).
- [15] S.R. Rastogi and N.J. Wagner, J. Chem. Phys. **104**, 9234 (1996).
- [16] G. Szamel, J. Chem. Phys. **114**, 8708 (2001).
- [17] W. Paul and D.Y. Yoon, Phys. Rev. E **52**, 2076 (1995); see also D.M. Heyes and A.C. Brańka, Mol. Phys. **98**, 1949 (2000).
- [18] Higher-order projections were examined by Hess and

- Hanley [19].
- [19] S. Hess and H.J.M Hanley, Phys. Rev. A **25**, 1801 (1982).
 - [20] H.J.M. Hanley, J.C. Rainwater and S. Hess, Phys. Rev. A **36**, 1795 (1987).
 - [21] X. Qiu, H.D. Ou-Yang, D.J. Pine and P. Chaikin, Phys. Rev. Lett. **61**, 2554 (1988).
 - [22] G. Szamel, J. Bławdziewicz and J.A. Leegwater, Phys. Rev. **45**, R2173 (1992).
 - [23] A.V. Indrani and S. Ramaswamy, Phys. Rev. E **52**, 6492 (1995).
 - [24] See also a related theoretical analysis: G. Szamel, Phys. Rev. Lett. **93**, 178301 (2004).
 - [25] L. Berthier, Phys. Rev. Lett. **98**, 220601 (2007).
 - [26] M. Krüger and M. Fuchs, Phys. Rev. Lett. **102**, 135701 (2009).
 - [27] T.K. Haxton and A.J. Liu, Phys. Rev. Lett. **99**, 195701 (2007).
 - [28] J. Delhommelle, J. Petravac, and D.J. Evans, Phys. Rev. E **68**, 031201 (2003); J. Delhommelle, Phys. Rev. E **71**, 016705 (2005); J. Delhommelle and J. Petravac, J. Chem. Phys. **123**, 074707 (2005).